

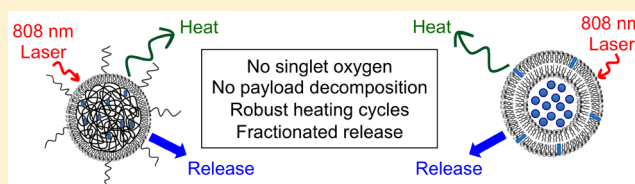
Clean Photothermal Heating and Controlled Release from Near-Infrared Dye Doped Nanoparticles without Oxygen Photosensitization

Samit Guha, Scott K. Shaw, Graeme T. Spence, Felicia M. Roland, and Bradley D. Smith*

Department of Chemistry and Biochemistry, University of Notre Dame, Notre Dame, Indiana 46556, United States

S Supporting Information

ABSTRACT: The photothermal heating and release properties of biocompatible organic nanoparticles, doped with a near-infrared croconaine (Croc) dye, were compared with analogous nanoparticles doped with the common near-infrared dyes ICG and IR780. Separate formulations of lipid–polymer hybrid nanoparticles and liposomes, each containing Croc dye, absorbed strongly at 808 nm and generated clean laser-induced heating (no production of $^1\text{O}_2$ and no photobleaching of the dye). In contrast, laser-induced heating of nanoparticles containing ICG or IR780 produced reactive $^1\text{O}_2$, leading to bleaching of the dye and also decomposition of coencapsulated payload such as the drug doxorubicin. Croc dye was especially useful as a photothermal agent for laser-controlled release of chemically sensitive payload from nanoparticles. Solution state experiments demonstrated repetitive fractional release of water-soluble fluorescent dye from the interior of thermosensitive liposomes. Additional experiments used a focused laser beam to control leakage from immobilized liposomes with very high spatial and temporal precision. The results indicate that fractional photothermal leakage from nanoparticles doped with Croc dye is a promising method for a range of controlled release applications.



1. INTRODUCTION

Laser-induced photothermal heating has many biomedical applications such as cell ablation,¹ drug release,² and gene delivery.³ The laser-absorbing chromophore can be either gold nanostructure,⁴ organic dye,⁵ carbon nanotube,⁶ inorganic nanoparticle,⁷ or polymeric material.⁸ There is a major technical advantage if the chromophore strongly absorbs in the near-infrared (NIR) window because NIR light penetrates furthest through skin and tissue.⁹ Gold nanostructures are popular choices for photothermal heating, but they have potential performance drawbacks such as irreversible morphology changes upon heating, slow rates of diffusion, and slow clearance from the body.¹⁰ On a per mass basis, organic dyes have the same photothermal heating capacity as gold nanostructures,¹¹ but most organic NIR dyes are limited by poor stability and photobleaching.¹² Typically, the photobleaching is due to a chemical reaction with reactive oxygen species (ROS) such as singlet oxygen ($^1\text{O}_2$) produced by energy transfer from the dye triplet excited state to nearby molecular oxygen which is known as type II reaction.¹³ In the type I reaction, the excited dye reacts directly with the substrate. Photothermal dyes that simultaneously emit heat and generate ROS are attractive for applications that aim to cause rapid cell death.¹⁴ However, certain photothermal applications are best conducted with chromophores that do not simultaneously generate ROS. Consider the process of photothermal release of chemically sensitive payloads, such as drugs, biologics, or oligonucleotides, where the concomitant production of ROS has the likely detrimental effect of causing payload decomposition. While many studies have demonstrated laser-triggered release of cargo

from nanoparticles, very few of them, if any, have evaluated if the released cargo is damaged.¹⁵

It is apparent that new classes of NIR organic dyes are needed for biomedical applications that require stable levels of clean photothermal heating over long periods of time or alternatively over repeated heating cycles. Recent reports have demonstrated that organic nanoparticles containing either porphyrin dye,¹⁶ gadolinium bis(naphthalocyanine) sandwich complex,¹⁷ or modified heptamethine indocyanine dye^{18,19} enable exclusive photothermal heating without photobleaching. In addition, there is recent evidence for laser-induced leakage from liposomes, containing a porphyrin chromophore, that does not involve bulk heating of the sample.²⁰ As a complement to these ongoing developments, we have discovered that croconaine (Croc) dyes (chemical structure in Figure 1) exhibit many of the desired features for high performance photothermal heating using a cheap 808 nm diode laser.^{21,22} In brief, Croc dyes absorb strongly at around 800 nm, and they have very short picosecond excited state lifetimes, low fluorescence quantum yields, and very little intersystem crossing to the excited triplet state. They efficiently convert 808 nm laser light into heat with negligible production of $^1\text{O}_2$. We have shown that Croc dyes can be encapsulated inside macrocyclic molecules and also within silicated micelles to give water-soluble nanoparticles with diameters <15 nm.²² In this present study, we address the need for larger, biocompatible organic

Received: May 22, 2015

Revised: June 26, 2015

Published: July 7, 2015

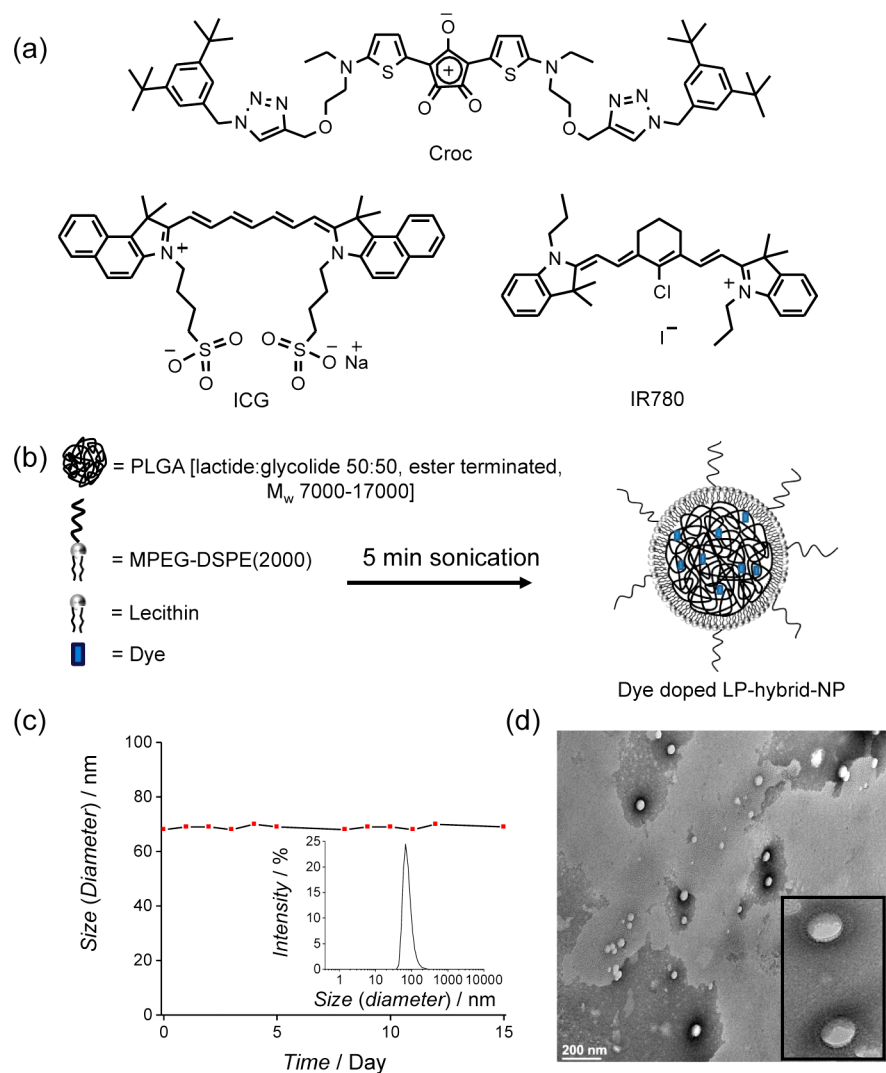


Figure 1. (a) Molecular structures of NIR dyes. (b) Schematic representation of dye doped LP-hybrid-NP fabrication. (c) DLS study of Croc/LP-hybrid-NP in HEPES buffer at pH 7.4. Hydrodynamic diameter 68 ± 1 nm and PDI = 0.109 (see inset) does not change over 15 days. (d) TEM image of Croc/LP-hybrid-NP; inset shows a 5 \times expansion of one section of the image.

nanoparticles with diameters of 50–200 nm that are commonly used for controlled release applications and have the potential to exploit the enhanced permeability and retention effect for tumor targeting.²³ Particles of this size are not likely to be excreted from the body so it is important to use biodegradable building blocks. We describe the construction of Croc doped lipid–polymer hybrid nanoparticles and Croc doped liposomes and show that both systems exhibit superior photothermal properties when compared to identical nanoparticle systems doped with two commonly used commercial NIR dyes: indocyanine green (ICG) and IR780 (structures in Figure 1a).^{24,25} We demonstrate how this high performance photothermal system permits new types of nanoparticle release strategies with very high levels of spatial and temporal control.

2. MATERIALS AND METHODS

2.1. Materials. The Croc dye used in this study was prepared using our published method²² and has the following photophysical properties in CHCl_3 : λ_{abs} 795 nm, ϵ $2.7 \times 10^5 \text{ M}^{-1} \text{ cm}^{-1}$, λ_{em} 810 nm, Φ_{F} 0.06.²² 2-[4-(2-Hydroxyethyl)piperazin-1-yl]ethanesulfonic acid (HEPES), PLGA [poly(DL-lactide-co-glycolide); lactide:glycolide 50:50, ester terminated, M_w 7000–17 000], cardiogreen [indocyanine green (ICG)], IR780 iodide, DPBF (1,3-diphenylisobenzofuran),

carboxyfluorescein (CF), and phosphotungstic acid were obtained from Sigma-Aldrich. Doxorubicin hydrochloride (DOX.HCl) was purchased from Fisher Scientific. 1-Palmitoyl-2-oleoyl-*sn*-glycero-3-phosphocholine (POPC) and 1,2-dipalmitoyl-*sn*-glycero-3-phosphocholine (DPPC) were purchased from Avanti Polar Lipids (USA) and stored in a freezer at -20 °C. *N*-(Carboxymethoxypoly(ethylene glycol)-2000)-1,2-distearoyl-*sn*-glycero-3-phosphoethanolamine, ammonium salt (MPEG-DSPE(2000)), was purchased from Corden Pharma (Switzerland) and stored in a freezer at -20 °C. Lecithin (90% Soybean) was purchased from Alfa Aesar and stored in a freezer at -20 °C. Singlet oxygen sensor green (SOSG) was purchased from Life Technologies (USA). Amicon Ultra (Ultra-15) centrifugal filter units with a molecular weight cutoff of 10 kDa were bought from Millipore (USA). Before opening, the chemicals were warmed to room temperature.

2.2. Lipid–Polymer Hybrid Nanoparticles (LP-Hybrid-NP).

2.2.1. Nanoparticle Preparation. Stock solutions for LP-hybrid-NP synthesis were MPEG-DSPE (2000): 1 mg/mL in 4 wt % ethanol:water solution; lecithin: 1 mg/mL in 4 wt % ethanol:water solution; PLGA: 2.5 mg/mL in acetonitrile. Stock solutions were stored at 4 °C and replaced after 3 weeks, with the exception of PLGA which was always prepared as a fresh solution. To synthesize LP-hybrid-NP, MPEG-DSPE(2000) stock (200 μL) and lecithin stock (12.5 μL) were added into deionized H_2O (3.7 mL). Solid organic dye (0.5 mg) was dissolved in the PLGA stock (400 μL) and was added

slowly dropwise. The resulting solution was sonicated using a probe sonicator for 5 min (sonicator frequency 20 kHz and power 130 W), which produced a clear solution. The solution was filtered and washed three times using Amicon Ultra-4 centrifugal filter [MWCO 10 kDa] and HEPES buffer at pH 7.4 [4000g, 30 min each time] to remove remaining organic solvent and free organic dye. The final weight ratio of components in the assembled nanoparticle was dye:DSPE-PEG(2000):lecithin:PLGA = 0.5:0.2:0.012:1.

2.2.2. Fluorescein and DOX Release from LP-Hybrid-NP. DOX and fluorescein release from Croc/DOX/LP-hybrid-NP and Croc/Fluorescein/LP-hybrid-NP was determined by a dialysis method using a dialysis membrane with 8 kDa MWCO (prevents passage of the nanoparticles) and HEPES (pH 7.4) as buffer. The sample in a cuvette was warmed to 37 °C for 2 min prior to irradiation for 15 min with an 808 nm diode laser which increased the sample temperature to 52 °C (control experiments did not laser irradiate). After laser irradiation the samples were incubated in the dark at 37 °C on a rotating incubator set at 200 rpm. At time points, the dialysate was taken out to estimate the amount of released fluorescein or DOX. Fluorescence intensity of DOX was measured at 591 nm when excited at 480 nm. Fluorescence intensity of fluorescein was measured at 512 nm when excited at 480 nm. All experiments were performed in triplicate. To achieve 100% release of fluorescein or DOX, the samples were treated with CH₃CN, which dissolved the nanoparticles. The percentage of release F (%) was calculated as $F(\%) = 100 \times (F_t - F_0) / (F_{\text{total}} - F_0)$, where F_t is the fluorescein or DOX intensity at the measured time point, F_0 is intensity at $t = 0$, and F_{total} is the intensity after treatment with CH₃CN.

2.3. Liposome Studies. **2.3.1. Liposome Preparation.** Appropriate ratios of POPC (10 mg/mL), DPPC (10 mg/mL), MPEG-DSPE(2000) (10 mg/mL), and Croc (1 mg/mL) in CHCl₃ were combined to give Croc/POPC (3:97) or Croc/MPEG-DSPE(2000)/DPPC (2:5:93). The solvent was removed by N₂ stream for 10 min, and the residual solvent was removed under high vacuum for 2 h to produce a Croc/lipid film. The lipid films were rehydrated with an appropriate amount of HEPES buffer (20 mM HEPES, 150 mM NaCl, pH 7.4) to give a final lipid + Croc concentration of 6.67 mM. After 1 h of incubation at $T > t_m$ of the lipid, the hydrated films were subjected to five freeze/thaw cycles (consisting of freezing the samples in liquid nitrogen followed by melting in a water bath to $T > t_m$ of the lipid). The disperse multilamellar vesicles were incubated at $T > t_m$ for 5 min, vortexed, and then extruded 21 times through a polycarbonate membrane (200 nm pore size, 19 mm diameter, Whatman nuclepore track-etch membrane filtration products) using a Liposofast extruder (Avestin, Ottawa, Canada) at $T > t_m$ to produce a suspension of unilamellar vesicles. The unincorporated Croc dye was removed by size exclusion using a column filled with Sephadex G-25 Superfine gel and cold HEPES buffer as eluent. An analogous procedure was used to make liposomes containing IR780 or DPBF in place of Croc.

2.3.2. Carboxyfluorescein Release Assay. Unilamellar vesicles were prepared with a lipid composition of thermosensitive Croc/MPEG-DSPE(2000)/DPPC (2:5:93) or nonthermosensitive Croc/POPC (3:97) using the procedure above, except the film was hydrated with carboxyfluorescein (CF) solution (50 mM CF, 20 mM HEPES, 100 mM NaCl at pH 7.4). The unencapsulated CF and Croc were removed by size exclusion using a column filled with Sephadex G-25 Superfine gel and cold HEPES buffer as eluent. CF is self-quenched at high concentrations inside the liposomes. An increase in CF fluorescence indicates release of CF from the vesicles into solution. Addition of 1% (w/v) Triton X-100 lyses the vesicles and releases the CF, allowing for normalization to 100% leakage. The percentage of CF release was calculated from the fluorescence intensity (Ex: 492 nm; Em: 517 nm) using the equation $F(\%) = 100 \times (F_t - F_0) / (F_{\text{total}} - F_0)$, where F_t is the CF intensity at the measured time point, F_0 is intensity at $t = 0$, and F_{total} is the intensity after treatment with Triton X-100. The laser triggered liposome release experiments in solution used a 808 nm diode laser (6 W/cm²) to heat microwells containing the samples. The nonthermosensitive formulation of Croc:POPC (3:97) is in a liquid crystalline phase before laser heating, and so although laser irradiation produces substantial photothermal heating

there is no membrane phase transition and no enhanced leakage of CF.

2.4. Photothermal Heating of Immobilized Liposomes in a Gel. Separate 60 × 15 mm Petri dishes were loaded with a suspension of gelatin (7 mL, 50 mg/mL) containing CF-loaded Croc/MPEG-DSPE(2000)/DPPC (2:5:93) liposomes (1.2 mL) at 30 °C. The Petri dishes containing the gelatin/liposome suspension were allowed to sit for 3 h at 15 °C, creating a robust gel, and then localized spots (4 mm²) on the gel surface were irradiated with an 808 nm diode laser (15 W/cm²). Four spots on one gel surface were irradiated continuously for 30, 60, 90, or 120 s, and the temperature at the end of each heating period was measured using a thermal imaging camera (ICL, USA). The four spots on the other gel surface were irradiated for a designated number of heating cycles, where each cycle consisted of laser irradiation for 15 s (which raised the temperature of the spot to 41 °C) followed by a 60 s break in laser heating. Fluorescence images of the released CF in the irradiated spots were captured using a Lumina IVIS machine (PerkinElmer, USA) with GFP excitation and emission filter sets and a 1 s acquisition time. Images were processed using ImageJ, and the uniform fluorescence of the nonirradiated gel was subtracted as background. Region of interest (ROI) analyses measured total and mean pixel intensity within each ROI.

3. RESULTS AND DISCUSSION

The study compared the photothermal heating properties of lipid-polymer hybrid nanoparticles and liposomes that were doped with the three different NIR dyes in Figure 1a. To help the reader, the two nanoparticle systems are described using a short systematic nomenclature that starts with the name of dye followed by the other composites. For example, Croc doped lipid-polymer hybrid nanoparticles are named Croc/LP-hybrid-NP, and Croc doped POPC liposomes are named Croc/POPC. The work is presented in the following sequence. First, a comparison of the dye doped lipid-polymer hybrid nanoparticles reveals the superior ability of Croc/LP-hybrid-NP to undergo clean photothermal heating without generating ROS. Then there is a demonstration of laser activated photothermal release of molecular payload from Croc doped lipid-polymer hybrid NP and thermosensitive liposomes.

3.1. Fabrication and Characterization of Dye Doped LP-Hybrid-NP. A rapid and straightforward literature sonication procedure was used to prepare the LP hybrid NP as a core-shell architecture with a hydrophobic core of PLGA [ester terminated poly(lactic-co-glycolic acid)] coated by a monolayer of two polar lipids: lecithin and MPEG-DSPE(2000) (Figure 1b; Figures S1 and S2).²⁶ It is worth noting that all three substances are approved for use in humans by the US FDA. The hydrophobic core readily accommodates additional hydrophobic molecules such as drugs or dyes.^{27–29} The PEG(2000) chains protruding from the surrounding shell form a protective corona that sterically protects the nanoparticles from self-aggregation and undesired interaction with biological surfaces. All nanoparticle preparations exhibited a narrow size distribution. Figure 1c shows representative DLS data for nanoparticles doped with Croc dye (Croc/LP-hybrid-NP), indicating a high level monodispersity [polydispersity index (PDI) = 0.109] and a particle diameter of 68 ± 1 nm in HEPES buffer at pH 7.4. Stock solutions of the nanoparticles could be stored for more than 15 days with no change in particle size distribution.

Transmission electron microscopy (TEM) was used to visualize the morphology of Croc/LP-hybrid-NP that had been deposited on a carbon-coated copper grid (300 mesh) and stained with 2% (w/v) phosphotungstic acid. The TEM images

show well-ordered and almost uniform spherical structures with average diameters of 65 nm (Figure 1d). The negative staining indicates higher contrast on the circumference of the polymeric nanoparticles consistent with a polymer core and a surrounding monolayer of polar lipid. Absorption spectra of the Croc/LP-hybrid-NP show two bands at 800 and 720 nm (Figure 2b).

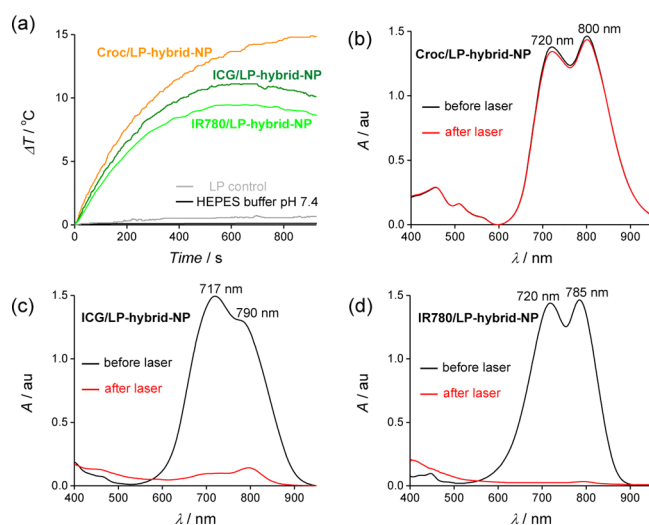


Figure 2. (a) Sample temperature profiles during laser irradiation (808 nm) for Croc/LP-hybrid-NP (orange), ICG/LP-hybrid-NP (deep green), and IR780/LP-hybrid-NP (light green) in HEPES buffer at pH 7.4. Control experiments: LP-hybrid-NP without any dye at pH 7.4 (HEPES buffer) (gray) and HEPES buffer alone at pH 7.4 (black). (b–d) UV/vis absorption of Croc/LP-hybrid-NP, ICG/LP-hybrid-NP, and IR780/LP-hybrid-NP, respectively, at pH 7.4 (HEPES buffer) before (black) and after (red) laser irradiation (15 min). Significant loss of ICG and IR780 absorption is observed after laser irradiation.

The peak at 720 nm is due to partial self-aggregation of Croc dye inside the particle. The amount of Croc self-aggregation inside the nanoparticles did not change significantly after sitting for 24 h, even when the solvent was 2% FBS (w/w) at pH 7.4 (HEPES buffer) (Figure S3a).

3.2. Photothermal Heating of Dye Doped LP-Hybrid-NP. For comparison studies, the following dye doped lipid-polymer hybrid NP were prepared using identical methods: Croc/LP-hybrid-NP, ICG/LP-hybrid-NP, and IR780/LP-hybrid-NP (for nanoparticle characterization data, see Figure S4). Separate cuvettes containing samples of each nanoparticle system in pH 7.4 HEPES buffer were irradiated for 15 min with an 808 nm diode laser, and the solution temperature was monitored with a thermocouple. In addition, absorption spectra of each sample were acquired before and after laser heating. As shown in Figure 2a, the solution temperature of the Croc/LP-hybrid-NP sample increased to a steady state of 15 °C above ambient, with minimal change in the Croc absorption spectrum. Additional laser irradiation experiments revealed a linear relationship between solution temperature increase and laser power (Figure S5). The remarkable stability of the Croc/LP-hybrid-NP to laser irradiation was further tested by repeating the irradiation experiments in 2% FBS (w/w), and there was no change in the photothermal behavior (Figure S3d). The results clearly indicate very high photostability and photothermal durability of Croc/LP-hybrid-NP.

The same laser heating experiments with ICG/LP-hybrid-NP and IR780/LP-hybrid-NP produced different heating results. The absorption spectra in Figure 2c,d and fluorescence spectra in Figure S6 show that 15 min of laser irradiation almost completely destroyed each dye's ability to absorb the 808 nm laser light. This time-dependent loss in absorption cross section explains why the maximum temperature increase is smaller (~10 °C for both systems) and also why there is a gradual decrease in sample temperature over the later stages of the laser irradiation (Figure 2a). This difference in dye photostability was readily apparent in cycling experiments that repeatedly irradiated the same sample. As shown in Figure 3, each sample

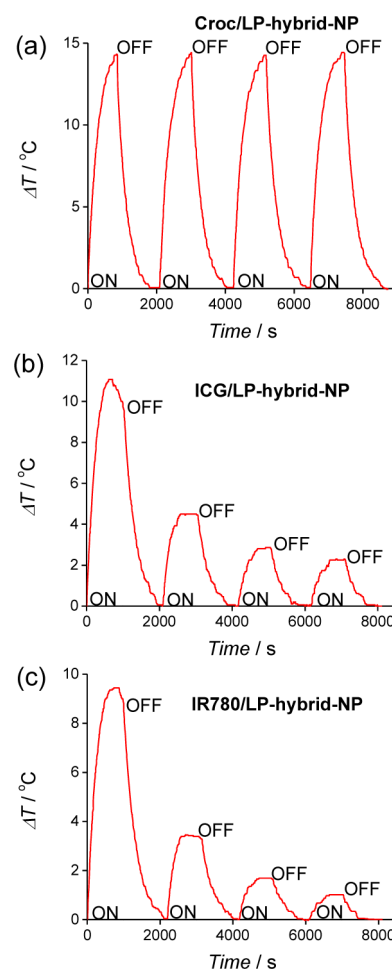


Figure 3. Four heating cycles of (a) Croc/LP-hybrid-NP, (b) ICG/LP-hybrid-NP, and (c) IR780/LP-hybrid-NP at pH 7.4 (HEPES buffer) with laser irradiation.

was subjected to four cycles of laser irradiation for 15 min followed by a break without light. The sample of Croc/LP-hybrid-NP showed no change in maximum temperature over the four iterations, whereas the samples of ICG/LP-hybrid-NP and IR780/LP-hybrid-NP exhibited a large decrease in photothermal heating after each irradiation step in the cycle. However, the size of the LP-hybrid-NPs was unchanged after several cycles of laser irradiation.

3.3. Oxygen Photosensitization by Dye Doped LP-Hybrid-NP. The photobleaching of ICG/LP-hybrid-NP and IR780/LP-hybrid-NP is consistent with generation of singlet oxygen ($^1\text{O}_2$) by dye photosensitization, and this hypothesis was confirmed by conducting two sets of chemical trapping

studies. The first set of studies incorporated the lipophilic organic compound 1,3-diphenylisobenzofuran (DPBF) within the core of the nanoparticles. DPBF is well-known to react quickly with $^1\text{O}_2$ to form a product with a decreased absorption maxima and associated fluorescence (Figure S7). The property makes DPBF an excellent chemical sensor for $^1\text{O}_2$ that is produced within the lipophilic core of a bilayer membrane or an organic nanoparticle.³⁰ Three analogous batches of the nanoparticles were prepared with DPBF and one of the three NIR dyes incorporated inside, i.e., ICG/DPBF/LP-hybrid-NP, IR780/DPBF/LP-hybrid-NP, and Croc/DPBF/LP-hybrid-NP (Figure S7). Each nanoparticle sample was irradiated for 15 min with an 808 nm laser, and the changes in DPBF fluorescence emission spectra (Figure S8) were recorded. In the case of Croc/DPBF/LP-hybrid-NP there were no spectral changes (Figure S8a), whereas the samples of ICG/DPBF/LP-hybrid-NP and IR780/DPBF/LP-hybrid-NP showed large decreases in the characteristic fluorescence emission peaks for DPBF at 453 and 477 nm (Figure S8b,c). This suggests that irradiation of ICG/DPBF/LP-hybrid-NP and IR780/DPBF/LP-hybrid-NP produced a significant amount of reactive $^1\text{O}_2$ that reacted with both the NIR dye and the DPBF $^1\text{O}_2$ sensor. Control experiments showed no bleaching of the dyes in the absence of laser irradiation. As expected, dye photobleaching led to diminished photothermal heating in the later stages of the irradiation experiments (Figure S9).

Another set of trapping experiments tested for the appearance of $^1\text{O}_2$ in the aqueous solution outside the nanoparticles. The $^1\text{O}_2$ sensor was the water-soluble fluorescent probe singlet oxygen sensor green (SOSG), which becomes highly fluorescent after reacting with $^1\text{O}_2$.³¹ Separate aqueous solutions of SOSG (pH 7.4) mixed with Croc/LP-hybrid-NP, ICG/LP-hybrid-NP, or IR780/LP-hybrid-NP were laser irradiated for 15 min. As expected, irradiation of the Croc/LP-hybrid-NP produced no change in SOSG emission, whereas irradiation of ICG/LP-hybrid-NP or IR780/LP-hybrid-NP produced large increases in SOSG emission indicating considerable $^1\text{O}_2$ production (Figure S10).

3.4. Photooxidation of Doxorubicin Encapsulated inside Dye Doped LP-Hybrid-NP. The significant differences in oxygen photosensitization prompted us to evaluate the effect of 808 nm laser irradiation on dye doped LP-hybrid-NP that also contained the anticancer drug doxorubicin (DOX).³² DOX is an effective topoisomerase II inhibitor and a fluorescent compound that is often utilized in clinical nanomedicine and preclinical studies.³³ The reactivity of DOX with ROS has not been examined in great detail. However, several studies have found that UV irradiation of solutions containing DOX and photosensitizers leads to destruction of the DOX.^{34–36} The degradation is indicated by a loss in the characteristic red fluorescence emission and greatly reduced DOX cytotoxicity. We conducted conceptually similar DOX degradation experiments by first preparing three separate batches of dye doped LP-hybrid-NP that also incorporated the lipophilic free base of DOX, i.e., ICG/DOX/LP-hybrid-NP, IR780/DOX/LP-hybrid-NP, and Croc/DOX/LP-hybrid-NP (Figure S11). Each NP system exhibited the characteristic DOX fluorescence emission bands at 559 and 591 nm when excited at 480 nm (Figure 4). The Croc/DOX/LP-hybrid-NP exhibited long storage stability and excellent photothermal heating performance (Figure S12), including negligible change in the DOX fluorescence intensity after laser irradiation for 15 min (Figure 4a,b). The ICG/DOX/LP-hybrid-NP and IR780/DOX/LP-hybrid-NP had a

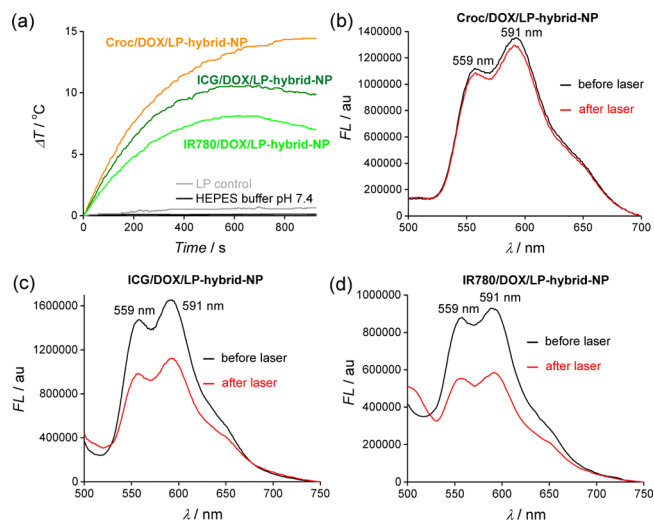


Figure 4. (a) Temperature change profiles during laser irradiation for Croc/DOX/LP-hybrid-NP (orange), ICG/DOX/LP-hybrid-NP (dark green), and IR780/DOX/LP-hybrid-NP (light green) at pH 7.4 (HEPES buffer). Control experiment: LP-hybrid-NPs without any dye at pH 7.4 (HEPES buffer) (gray) and HEPES buffer alone at pH 7.4 (black). (b–d) DOX fluorescence ($\lambda_{\text{ex}} = 480$ nm) in samples of Croc/DOX/LP-hybrid-NP, ICG/DOX/LP-hybrid-NP, and IR780/DOX/LP-hybrid-NP, respectively, before (black) and after (red) laser (15 min) irradiation. The DOX decrease in the three samples was 4%, 30%, and 35%, respectively.

comparable size and PDI (Figure S13). As expected, the laser heating performance was weaker, with evidence of significant dye photobleaching. Furthermore, there was a 30–35% loss in DOX fluorescence intensity after laser irradiation for 15 min (Figure 4c,d) presumably due to reaction with photogenerated $^1\text{O}_2$. The structures of the DOX decomposition products were not elucidated, but the literature clearly indicates that photooxidized DOX has greatly decreased therapeutic efficacy.³⁶

3.5. Laser-Promoted Release of Payload from LP-Hybrid-NP. The clean photothermal heating of Croc doped nanoparticles (i.e., no generation of destructive $^1\text{O}_2$) is very attractive for laser activated drug release applications. This possibility was first tested by measuring the effect of laser irradiation on the leakage of encapsulated molecular payload from Croc doped LP-hybrid-NP. A dialysis assay compared the rate of DOX escape from Croc/DOX/LP-hybrid-NP after the sample had been irradiated with 808 nm diode laser for 15 min (which increased the sample temperature to 52 °C) to a control sample that was kept entirely in the dark. As shown in Figure S14a, the half-life for DOX leakage from the nanoparticles in the dark was 18 h, and this was shortened to 6 h by 15 min of preliminary laser irradiation. DLS data indicated that the size of the NPs was unchanged after the laser irradiation (Figure S15). The same trend was observed in a separate dialysis experiment that encapsulated the fluorescent dye fluorescein (i.e., Croc/fluorescein/LP-hybrid-NP; see Figure S16). In this case, the half-life for fluorescein leakage from the nanoparticles in the dark was 8.5 h, and this was shortened to 4 h by 15 min of preliminary laser irradiation (Figure S14b). Thus, an initial 15 min period of laser irradiation was able to induce a modest increase in the relatively slow leakage rate of drug or dye payload from Croc/payload/LP-hybrid-NP. These leakage rates match those observed with other PLGA nanoparticle

systems.^{32,37} In order to explain the enhanced leakage, we determined the PLGA glass transition temperature (T_g) to be 42–46 °C (Figure S17). We hypothesize that laser-induced heating of the Croc/payload/LP-hybrid-NP induces a temporary thermal phase change in the PLGA core from a rigid, glassy state to a compliant, rubbery state, which facilitates diffusion of encapsulated payload toward the periphery of the nanoparticle. However, complete escape from the nanoparticle is still fairly slow since the payload has to diffuse through the surrounding shell, which is a densely packed monolayer of polar lipids.²⁷

3.6. Laser-Promoted Release of Payload from Thermosensitive Liposomes. Liposomes are effective biocompatible nanoparticle systems for drug delivery.³⁸ In the literature, there are different ways of creating thermosensitive liposomes.³⁹ One approach is to use membrane formulations that undergo a thermal phase transition of the saturated acyl chains in the bilayer membrane from gel to fluid phase leading to greatly enhanced leakage of aqueous contents from the liposomes.⁴⁰ There are only a few reports of thermosensitive liposomes that incorporate NIR dyes as the photothermal agent, in part because of anticipated problems due to dye photobleaching and oxygen photosensitization⁴¹ but also because of the emerging success using gold nanostructures to absorb the NIR light.⁴² While gold nanoparticles have many attractive features, some structures (such as nanorods) are known to undergo heat-driven morphology changes that alter their light absorption and limit their potential for applications that require repetitive photothermal heating.

To demonstrate the potential of Croc doped liposomes for laser-activated release of aqueous contents, thermosensitive liposomes were prepared with Croc dye in the lipophilic interior of the membrane and water-soluble carboxyfluorescein (CF) trapped in the aqueous interior. The release of CF from the liposomes is easily monitored by its increase in fluorescence intensity as it is diluted into the external solution (Figure 5a). Two liposome systems were studied: a nonthermosensitive formulation composed of Croc:POPC (3:97) and a thermosensitive formulation composed of Croc/MPEG-DSPE(2000)/DPPC (2:5:93) with a measured phase transition temperature of 42.2 °C (Figure S18). There was substantial leakage from the thermosensitive liposome system (Figure 5b). Furthermore, substantial CF leakage started when the bulk solution temperature passed through the membrane phase transition temperature (Figure 5b).

An attractive feature of this family of thermosensitive liposomes is the potential for fractionated release. That is the leakage stops if the sample temperature dips below the membrane phase transition temperature. The unique ability of Croc dye to undergo multiple photothermal heating cycles without loss of heating efficiency makes it attractive for methods that use repetitive doses of laser irradiation to achieve fractionated liposome leakage. Figure 6 shows the results of two sets of CF leakage experiments that demonstrate this concept. Figure 6a shows the controlled incremental CF release from thermosensitive Croc/MPEG-DSPE(2000)/DPPC (2:5:93) liposomes in aqueous solution due to repetitive 1 min doses of 808 nm laser irradiation with 10 min breaks. In Figure 6b,c is a more complex CF leakage experiment that highlights the spatial as well as the temporal attributes of a laser beam. Two Petri dishes were each partially filled with identical layers of a relatively rigid “gel” containing a homogeneous distribution of thermosensitive Croc/MPEG-DSPE(2000)/DPPC (2:5:93) liposomes that were loaded with CF. Preliminary tests showed

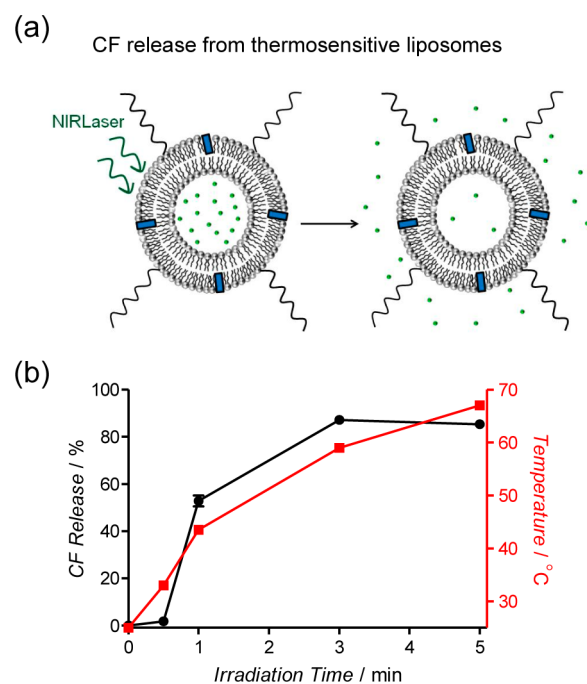


Figure 5. (a) Schematic representation of photothermal CF release from thermosensitive liposomes due to laser irradiation. (b) Photothermal CF release (black line) from Croc/MPEG-DPPE(2000)/DPPC (2:5:93) liposomes at pH 7.4 after laser (808 nm, 6 W/cm²) irradiation. The red line is the sample temperature.

that a relatively narrow 808 nm laser beam (4 mm²) directed at the gel surface produced a localized photothermal heating spot due to laser absorption by the Croc dye in the liposomes. Furthermore, the heating caused release of CF from the liposomes and the increased CF fluorescence at the heating spot could be observed by fluorescence imaging of the entire Petri dish. The first experiment (Figure 6b) used the laser beam to create four separate heating spots (A–D) with continuous laser irradiation times ranging from 30 to 120 s. As shown by the associated bar graph in Figure 6d, a longer laser irradiation time produced a commensurate increase in local CF leakage. The second experiment used the same laser beam, but this time the photothermal heating at a single spot was cycled a specified number of times, with each cycle involving 15 s of laser and 60 s of dark. The four spots in Figure 6c (E–H) correspond to 1–4 photothermal heating cycles, respectively. The associated graph in Figure 6e shows that the amount of local CF leakage increased almost linearly with the number of heating cycles. The high photostability of the Croc dye is the key attribute that allowed this fractionated liposome leakage of CF over multiple cycles. This type of repetitive release cannot be achieved with thermosensitive liposomes containing ICG or IR780 because they quickly photobleach.

Comparison of Figures 6b and 6c shows that fractionated photothermal heating is an effective way to minimize the thermal diffusion of leaked CF from the spot of heating. The effect is nicely illustrated by comparing the wider zone of released CF in spot B (diameter 10 mm, spot irradiated constantly for 60 s which produced a maximum temperature of 56 °C) with smaller spot H (diameter 3.6 mm, spot irradiated four times for 15 s with 1 min breaks, each heating cycle only reached a maximum temperature of 41 °C). Both spots received the same total dose of laser photons, but there was less thermal diffusion of the released CF in spot H due to the

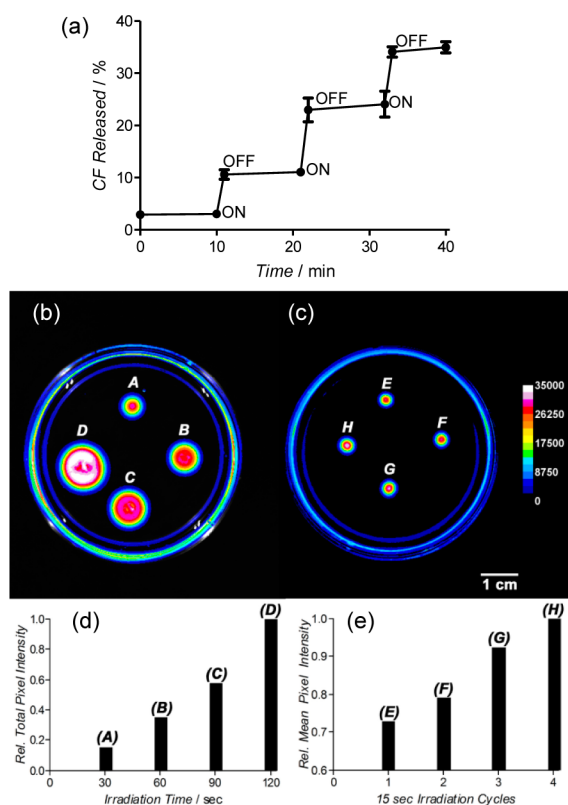


Figure 6. (a) Fractionated laser-induced photothermal release of CF from thermosensitive liposomes made of Croc/MPEG-DPPE(2000)/DPPC (2:5:93) in a solution of HEPES buffer (pH 7.4). (b) Fluorescence image of a Petri dish holding a gel with an even distribution of immobilized Croc/MPEG-DSPE(2000)/DPPC (2:5:93) liposomes. The four fluorescent spots indicate CF release due to continuous laser (808 nm, 15 W/cm²) irradiation of a 4 mm² zone for the following time periods and final temperatures: (A) 30 s, 50 °C; (B) 60 s, 56 °C; (C) 90 s, 57 °C; (D) 120 s, 59 °C. (c) Fluorescence image of an identical Petri dish holding a gel with an even distribution of immobilized Croc/MPEG-DSPE(2000)/DPPC (2:5:93) liposomes. The four fluorescent spots indicate CF release due to laser (808 nm, 15 W/cm²) irradiation of a 4 mm² zone for the following cycles of 15 s irradiation followed by 60 s break, (E) 1 cycle, (F) 2 cycles, (G) 3 cycles, and (H) 4 cycles. Each 15 s heating period raised the temperature of the spot to 41 °C. (d) Comparison of relative total fluorescence pixel intensity of the four spots in image (b). (e) Comparison of relative mean fluorescence pixel intensity of the four spots in image (c).

fractionated irradiation which allowed a cooling period between each irradiation. These simple experiments indicate how clean (i.e., no production of undesired ¹O₂) and fractionated photothermal release of payload from thermosensitive liposomes containing highly photostable Croc dye can be combined with the precise spatial precision of a laser beam for various types of controlled release applications. For example, we envision possible methods in nanomedicine that immobilize Croc-containing thermosensitive liposomes in superficial *in vivo* locations (e.g., tattooed under the skin⁴³) and use focused laser beam irradiation to trigger predictable amounts of leaked pharmaceutical over time. This method is attractive for situations that need to maintain dosage levels within an optimal therapeutic window. It may be possible to automate the process by connecting the repetitive laser heating to a diagnostic feedback system that monitors the level of the released payload in the external media.

4. CONCLUSIONS

Croc dye has several attractive photothermal properties. It absorbs strongly at 808 nm, a highly effective NIR wavelength for biological optical applications, and generates clean laser-induced heating (no generation of ¹O₂) without photobleaching of the dye. In contrast, laser-induced heating of nanoparticles that contain the common commercial NIR dyes ICG or IR780 simultaneously produces reactive ¹O₂, which leads to bleaching of the dye and also decomposition of coencapsulated payload such as the drug doxorubicin. Croc doped lipid-polymer hybrid nanoparticles have several favorable features for effective photothermal therapy.^{44,45} The nanoparticles are fabricated by a straightforward, rapid, and reproducible sonication method, and all of the nanoparticle components (except the Croc dye) are approved by the US FDA for use in humans. The special ability of Croc doped lipid-polymer nanoparticles to produce consistent photothermal heating over multiple heating cycles should enable future development of alternative strategies in photothermal therapy, such as repetitive fractionated heating of tumors⁴⁶ or photothermally enhanced uptake of chemotherapeutics.⁴⁷ Croc dye is especially useful for repetitive fractional release of water-soluble payload from the interior of thermosensitive liposomes. While the shallow penetration of NIR light through skin and tissue is a technical limitation for certain biomedical applications, the precise spatial and temporal control of a laser beam compares favorably with other methods used to induce hyperthermia.⁴⁸

■ ASSOCIATED CONTENT

Supporting Information

Chemical structures, schematic summaries of experimental methods, and additional data. The Supporting Information is available free of charge on the ACS Publications website at DOI: 10.1021/acs.langmuir.5b01878.

■ AUTHOR INFORMATION

Corresponding Author

*E-mail: smith.115@nd.edu (B.D.S.).

Notes

The authors declare no competing financial interest.

■ ACKNOWLEDGMENTS

We are grateful for funding support from the Walther Cancer Foundation Advancing Basic Cancer Research Grant (2013/14) administered by the Harper Cancer Research Institute (USA), the NSF, and NIH Grants R01GM059078 (B.D.S.) and T32GM075762 (S.K.S. and F.M.R.).

■ ABBREVIATIONS

Croc, croconaine; ICG, indocyanine green; IR780 iodide, 2-[2-chloro-3-[(1,3-dihydro-3,3-dimethyl-1-propyl-2H-indol-2-ylidene)ethylidene]-1-cyclohexen-1-yl]ethenyl]-3,3-dimethyl-1-propylindolium iodide; NIR, near-infrared; TEM, transmission electron microscopy; DLS, dynamic light scattering; DSC, differential scanning calorimetry; HEPES, 2-[4-(2-hydroxyethyl)piperazin-1-yl]ethanesulfonic acid; PLGA, [poly-(DL-lactide-co-glycolide)]; DPBF, 1,3-diphenylisobenzofuran; SOSG, singlet oxygen sensor green; CF, carboxyfluorescein; DOX, doxorubicin; POPC, 1-palmitoyl-2-oleoyl-*sn*-glycero-3-phosphocholine; DPPC, 1,2-dipalmitoyl-*sn*-glycero-3-phosphocholine; MPEG-DSPE(2000), *N*-(carboxymethoxypoly-

(ethylene glycol)-2000)-1,2-distearoyl-*sn*-glycero-3-phosphoethanolamine, ammonium salt; $^1\text{O}_2$, singlet oxygen; PDI, polydispersity index; ROS, reactive oxygen species.

REFERENCES

- (1) Lal, S.; Clare, S. E.; Halas, N. J. Nanoshell-Enabled Photothermal Cancer Therapy: Impending Clinical Impact. *Acc. Chem. Res.* **2008**, *41*, 1842–1851.
- (2) Leung, S. J.; Romanowski, M. NIR-Activated Content Release from Plasmon Resonant Liposomes for Probing Single-Cell Responses. *ACS Nano* **2012**, *6*, 9383–9391.
- (3) Huschka, R.; Barhoumi, A.; Liu, Q.; Roth, J. A.; Ji, L.; Halas, N. J. Gene Silencing by Gold Nanoshell-Mediated Delivery and Laser-Triggered Release of Antisense Oligonucleotide and siRNA. *ACS Nano* **2012**, *6*, 7681–7691.
- (4) Hauck, T. S.; Jennings, T. L.; Yatsenko, T.; Kumaradas, J. C.; Chan, W. C. Enhancing the Toxicity of Cancer Chemotherapeutics with Gold Nanorod Hyperthermia. *Adv. Mater.* **2008**, *20*, 3832–3838.
- (5) Yuan, A.; Wu, J.; Tang, X.; Zhao, L.; Xu, F.; Hu, Y. Application of Near-Infrared Dyes for Tumor Imaging, Photothermal, and Photodynamic Therapies. *J. Pharm. Sci.* **2013**, *102*, 6–28.
- (6) Moon, H. K.; Lee, S. H.; Choi, H. C. In Vivo Near-Infrared Mediated Tumor Destruction by Photothermal Effect of Carbon Nanotubes. *ACS Nano* **2009**, *3*, 3707–3713.
- (7) Jaque, D.; Martinez Maestro, L.; del Rosal, B.; Haro-Gonzalez, P.; Benayas, A.; Plaza, J. L.; Rodriguez, E. M.; Solé, J. G. Nanoparticles for Photothermal Therapies. *Nanoscale* **2014**, *6*, 9494–9530.
- (8) Cheng, L.; Yang, K.; Chen, Q.; Liu, Z. Organic Stealth Nanoparticles for Highly Effective in Vivo Near-Infrared Photothermal Therapy of Cancer. *ACS Nano* **2012**, *6*, 5605–5613.
- (9) Parrish, J. A. New Concepts in Therapeutic Photomedicine; Photochemistry, Optical Targeting and the Therapeutic Window. *J. Invest. Dermatol.* **1981**, *77*, 45–50.
- (10) Khlebtsov, N.; Dykman, L. Biodistribution and Toxicity of Engineered Gold Nanoparticles: A Review of in Vitro and in Vivo Studies. *Chem. Soc. Rev.* **2011**, *40*, 1647–1671.
- (11) Jiang, R.; Cheng, S.; Shao, L.; Ruan, Q.; Wang, J. Mass-Based Photothermal Comparison Among Gold Nanocrystals, PbS Nanocrystals, Organic Dyes, and Carbon Black. *J. Phys. Chem. C* **2013**, *117*, 8909–8915.
- (12) Engel, E.; Schraml, R.; Maisch, T.; Kobuch, K.; König, B.; Szeimies, R.-M.; Hillenkamp, J.; Bäuml, W.; Vasold, R. Light-Induced Decomposition of Indocyanine Green. *Invest. Ophthalmol. Visual Sci.* **2008**, *49*, 1777–1783.
- (13) Sheng, Z.; Hu, D.; Zheng, M.; Zhao, P.; Liu, H.; Gao, D.; Gong, P.; Gao, G.; Zhang, P.; Ma, Y.; Cai, L. Smart Human Serum Albumin-Indocyanine Green Nanoparticles Generated by Programmed Assembly for Dual-Modal Imaging-Guided Cancer Synergistic Phototherapy. *ACS Nano* **2014**, *8*, 12310–12322.
- (14) Guo, M.; Mao, H.; Li, Y.; Zhu, A.; He, H.; Yang, H.; Wang, Y.; Tian, X.; Ge, C.; Peng, Q.; Wang, X.; Yang, X.; Chen, X.; Liu, G.; Chen, H. Dual Imaging-guided Photothermal/Photodynamic Therapy Using Micelles. *Biomaterials* **2014**, *35*, 4656–4666.
- (15) Wan, Z.; Mao, H.; Guo, M.; Li, Y.; Zhu, A.; Yang, H.; He, H.; Shen, J.; Zhou, L.; Jiang, Z.; Ge, C.; Chen, X.; Yang, X.; Liu, G.; Chen, H. Highly Efficient Hierarchical Micelles Integrating Photothermal Therapy and Singlet Oxygen-Synergized Chemotherapy for Cancer Eradication. *Theranostics* **2014**, *4*, 399–411.
- (16) MacDonald, T. D.; Liu, T. W.; Zheng, G. An MRI-Sensitive, Non-Photobleachable Porphyrin Photothermal Agent. *Angew. Chem., Int. Ed.* **2014**, *53*, 6956–6959.
- (17) Mathew, S.; Murakami, T.; Nakatsuji, H.; Okamoto, H.; Morone, N.; Heuser, J. E.; Hashida, M.; Imahori, H. Exclusive Photothermal Heat Generation by a Gadolinium Bis-(naphthalocyanine) Complex and Inclusion into Modified High-Density Lipoprotein Nanocarriers for Therapeutic Applications. *ACS Nano* **2013**, *7*, 8908–8916.
- (18) Cheng, L.; He, W.; Gong, H.; Wang, C.; Chen, Q.; Cheng, Z.; Liu, Z. PEGylated Micelle Nanoparticles Encapsulating a Non-Fluorescent Near-Infrared Organic Dye as a Safe and Highly-Effective Photothermal Agent for In Vivo Cancer Therapy. *Adv. Funct. Mater.* **2013**, *23*, 5893–5902.
- (19) Gong, H.; Dong, Z.; Liu, Y.; Yin, S.; Cheng, L.; Xi, W.; Xiang, J.; Liu, K.; Li, Y.; Liu, Z. Engineering of Multifunctional Nano-Micelles for Combined Photothermal and Photodynamic Therapy Under the Guidance of Multimodal Imaging. *Adv. Funct. Mater.* **2014**, *24*, 6492–6502.
- (20) Carter, K. A.; Shao, S.; Hoopes, M. I.; Luo, D.; Ahsan, B.; Grigoryants, V. M.; Song, W.; Huang, H.; Zhang, G.; Pandey, R. K.; Geng, J.; Pfeifer, B. A.; Scholes, C. P.; Ortega, J.; Karttunen, M.; Lovell, J. F. Porphyrin–Phospholipid Liposomes Permeabilized by Near-Infrared Light. *Nat. Commun.* **2014**, *5*, 3546.
- (21) Spence, G. T.; Hartland, G. V.; Smith, B. D. Activated Photothermal Heating Using Croconaine Dyes. *Chem. Sci.* **2013**, *4*, 4240–4244.
- (22) Spence, G. T.; Lo, S. S.; Ke, C.; Destecroix, H.; Davis, A. P.; Hartland, G. V.; Smith, B. D. Near-Infrared Croconaine Rotaxanes and Doped Nanoparticles for Enhanced Aqueous Photothermal Heating. *Chem. - Eur. J.* **2014**, *20*, 12628–12635.
- (23) Iyer, A. K.; Khaled, G.; Fang, J.; Maeda, H. Exploiting the Enhanced Permeability and Retention Effect for Tumor Targeting. *Drug Discovery Today* **2006**, *11*, 812–818.
- (24) Yu, J.; Javier, D.; Yaseen, M. A.; Nitin, N.; Richards-Kortum, R.; Anvari, B.; Wong, M. S. Self-Assembly Synthesis, Tumor Cell Targeting, and Photothermal Capabilities of Antibody-Coated Indocyanine Green Nanocapsules. *J. Am. Chem. Soc.* **2010**, *132*, 1929–1938.
- (25) Zhang, E.; Luo, S.; Tan, X.; Shi, C. Mechanistic Study of IR-780 Dye as a Potential Tumor Targeting and Drug Delivery Agent. *Biomaterials* **2014**, *35*, 771–778.
- (26) Fang, R. H.; Aryal, S.; Hu, C.-M. J.; Zhang, L. Quick Synthesis of Lipid-Polymer Hybrid Nanoparticles with Low Polydispersity Using a Single-Step Sonication Method. *Langmuir* **2010**, *26*, 16958–16962.
- (27) Zhang, L.; Chan, J. M.; Gu, F. X.; Rhee, J.-W.; Wang, A. Z.; Radovic-Moreno, A. F.; Alexis, F.; Langer, R.; Farokhzad, O. C. Self-Assembled Lipid-Polymer Hybrid Nanoparticles: A Robust Drug Delivery Platform. *ACS Nano* **2008**, *2*, 1696–1702.
- (28) Chan, J. M.; Zhang, L.; Yuet, K. P.; Liao, G.; Rhee, J.-W.; Langer, R.; Farokhzad, O. C. PLGA–Lecithin–PEG Core–Shell Nanoparticles for Controlled Drug Delivery. *Biomaterials* **2009**, *30*, 1627–1634.
- (29) Raemdonck, K.; Braeckmans, K.; Demeester, J.; De Smedt, S. C. Merging the Best of Both Worlds: Hybrid Lipid-Enveloped Matrix Nanocomposites in Drug Delivery. *Chem. Soc. Rev.* **2014**, *43*, 444–472.
- (30) Wozniak, M.; Tanfani, F.; Bertoli, E.; Zolese, G.; Antosiewicz, J. A New Fluorescence Method to Detect Singlet Oxygen Inside Phospholipid Model Membranes. *Biochim. Biophys. Acta, Lipids Lipid Metab.* **1991**, *1082*, 94–100.
- (31) Lin, H.; Shen, Y.; Chen, D.; Lin, L.; Wilson, B. C.; Li, B.; Xie, S. Feasibility Study on Quantitative Measurements of Singlet Oxygen Generation Using Singlet Oxygen Sensor Green. *J. Fluoresc.* **2013**, *23*, 41–47.
- (32) Zheng, M.; Yue, C.; Ma, Y.; Gong, P.; Zhao, P.; Zheng, C.; Sheng, Z.; Zhang, P.; Wang, Z.; Cai, L. Single-Step Assembly of DOX/ICG Loaded Lipid-Polymer Nanoparticles for Highly Effective Chemo-Photothermal Combination Therapy. *ACS Nano* **2013**, *7*, 2056–2067.
- (33) Ang, C. Y.; Tan, S. Y.; Zhao, Y. L. Recent Advances in Biocompatible Nanocarriers for Delivery of Chemotherapeutic Cargoes Towards Cancer Therapy. *Org. Biomol. Chem.* **2014**, *12*, 4776–4806.
- (34) Chen, M.; Hein, S.; Le, D. Q. S.; Feng, W.; Foss, M.; Kjems, J.; Besenbacher, F.; Zou, X.; Bünger, C. Free Radicals Generated by Tantalum Implants Antagonize the Cytotoxic Effect of Doxorubicin. *Int. J. Pharm.* **2013**, *448*, 214–220.

(35) Ramu, A.; Mehta, M. M.; Leaseburg, T.; Aleksic, A. The Enhancement of Riboflavin-Mediated Photo-oxidation of Doxorubicin by Histidine and Urocanic Acid. *Cancer Chemother. Pharmacol.* **2001**, *47*, 338–346.

(36) Ramu, A.; Mehta, M. M.; Liu, J.; Turyan, I.; Aleksic, A. The Riboflavin-Mediated Photooxidation of Doxorubicin. *Cancer Chemother. Pharmacol.* **2000**, *46*, 449–458.

(37) Yang, J.; Lee, J.; Kang, J.; Oh, S. J.; Ko, H.-J.; Son, J.-H.; Lee, K.; Suh, J.-S.; Huh, Y.-M.; Haam, S. Smart Drug-Loaded Polymer Gold Nanoshells for Systemic and Localized Therapy of Human Epithelial Cancer. *Adv. Mater.* **2009**, *21*, 4339–4342.

(38) Torchilin, V. P. Recent Advances with Liposomes as Pharmaceutical Carriers. *Nat. Rev. Drug Discovery* **2005**, *4*, 145–60.

(39) Leung, S. J.; Romanowski, M. Light-Activated Content Release from Liposomes. *Theranostics* **2012**, *2*, 1020–1036.

(40) Li, L.; ten Hagen, T. L. M.; Schipper, D.; Wijnberg, T. M.; van Rhoon, G. C.; Eggermont, A. M. M.; Lindner, L. H.; Koning, G. A. Triggered Content Release from Optimized Stealth Thermosensitive Liposomes Using Mild Hyperthermia. *J. Controlled Release* **2010**, *143*, 274–279.

(41) Giraudeau, C.; Moussaron, A.; Stallivieri, A.; Mordon, S.; Frochot, C. Indocyanine Green: Photosensitizer or Chromophore? Still a Debate. *Curr. Med. Chem.* **2014**, *21*, 1871–1897.

(42) You, J.; Zhang, P.; Hu, F.; Du, Y.; Yuan, H.; Zhu, J.; Wang, Z.; Zhou, J.; Li, C. Near-Infrared Light-Sensitive Liposomes for the Enhanced Photothermal Tumor Treatment by the Combination with Chemotherapy. *Pharm. Res.* **2014**, *31*, 554–565.

(43) Shio, M. T.; Paquet, M.; Martel, C.; Bosschaerts, T.; Stienstra, S.; Olivier, M.; Fortin, A. Drug Delivery by Tattooing to Treat Cutaneous Leishmaniasis. *Sci. Rep.* **2014**, *4*, 4156.

(44) Jaque, D.; Martinez Maestro, L.; del Rosal, B.; Haro-Gonzalez, P.; Benayas, A.; Plaza, J. L.; Rodríguez, E. M.; Solé, J. G. Nanoparticles for Photothermal Therapies. *Nanoscale* **2014**, *6*, 9494–9530.

(45) Devadas, M. S.; Devkota, T.; Guha, S.; Shaw, S. K.; Smith, B. D.; Hartland, G. V. Spatial Modulation Spectroscopy for Imaging and Quantitative Analysis of Single Dye-doped Organic Nanoparticles Inside Cells. *Nanoscale* **2015**, *7*, 9779–9785.

(46) Gutwein, L. G.; Singh, A. K.; Hahn, M. A.; Rule, M. C.; Knapik, J. A.; Moudgil, B. M.; Brown, S. C.; Grobmyer, S. R. Fractionated Photothermal Antitumor Therapy with Multidye Nanoparticles. *Int. J. Nanomed.* **2012**, *7*, 351–357.

(47) Tian, B.; Wang, C.; Zhang, S.; Feng, L.; Liu, Z. Photothermally Enhanced Photodynamic Therapy Delivered by Nano-Graphene Oxide. *ACS Nano* **2011**, *5*, 7000–7009.

(48) Mura, S.; Nicolas, J.; Couvreur, P. Stimuli-Responsive Nanocarriers for Drug Delivery. *Nat. Mater.* **2013**, *12*, 991–1003.